

ADVANCES IN APPLICATION OF PROPER ORTHOGONAL DECOMPOSITION IN INVERSE PROBLEMS

Z. OSTROWSKI¹, R.A. BIALECKI¹ and A.J. KASSAB²

¹ *Silesian University of Technology, Institute of Thermal Technology, ul.Konarskiego 22, 44-100 Gliwice, Poland*

e-mail: ostry@polsl.pl, bialecki@itc.polsl.pl

² *University of Central Florida, Department of Mechanical, Materials & Aerospace Engineering, PO Box 162450, Orlando, FL 32816-2450, USA*

e-mail: kassab@mail.ucf.edu

Abstract - Some recent advances in the application of the Proper Orthogonal Decomposition (POD) in inverse analysis of steady state heat conduction problems are presented. The developed technique is aimed at retrieving both the distribution of the convective heat transfer coefficients and the heat conductivities of the constituent materials. The idea is to solve a sequence of direct problems within the body under consideration to construct a reduced model. POD used at this stage serves two purposes: reduces the number of DOFs necessary to describe the spatial distribution of the temperature and regularizes the inverse problems by filtering out the noise. At the first step each retrieved parameter is sampled at several levels in the vicinity of the predicted solution. Then a sequence of direct problems is solved for all combinations of the sampled parameters. The resulting temperature fields at a predefined set of internal and boundary points is obtained using the Finite Element Method (FEM). POD technique applied to this sequence of discrete temperature fields produces a set of uncorrelated vectors (POD basis). The temperature field is then approximated by a low-order model defined as a sum of the POD basis vectors multiplied by unknown POD amplitudes. The latter are expressed as a linear combination of the Radial Basis Functions (RBFs) depending on the retrieved parameters. The unknown coefficients of this combination are evaluated from the condition that the low-order model should exactly reproduce the snapshots. Finally, the sought after parameters are determined by least-square fit of the low-order model to the measurement data. Numerical example shows the robustness and numerical stability of the scheme. The technique is shown to be insensitive to the measurement errors, and capable of producing a stable solution even in presence of large errors.

1. INTRODUCTION

The history of POD was started over 100 years ago by the work of Pearson [15]. At that time POD was used as a tool of processing statistical data. Since then the technique was several times re-developed in various fields including: signal processing and control theory [10], fluid flow and dynamics, turbulence [1, 3, 7], human face recognition [8], process identification, adaptive control, image processing, pattern recognition, weather prediction, oceanography, data compression, neural activity, and many others. Depending on the area of application the method is known under several names: Karhunen-Loeve Decomposition (KLD), Principal Component Analysis (PCA) or Singular Value Decomposition (SVD) are just few of them. Some more recent description of POD theory can be found in [9, 19].

The aim of using POD in inverse analysis is to find the correlation between solutions of direct problems corresponding to a certain set of assumed values of the parameters to be retrieved. POD produces low-order high quality approximation of the field under consideration. The side effect of the application of POD in inverse analysis is the filtration of the noise in the temperature fields.

The paper presents a novel application of POD in inverse analysis, namely the possibility of simultaneous estimation of film coefficient distribution and heat conductivity of a body of complex shape composed of several materials. As in our previous papers [4, 13], the proposed technique uses POD as a regularization tool. This feature of POD results from its ability of reducing the number of unknowns, without losing the accuracy. Reduction of DOFs is a well known and efficient technique of filtering out higher frequency errors being an essential mean of achieving stability of every inverse algorithm [2, 14, 17]. An arbitrary solution of the direct problem can then be expressed as a linear combination of only few basis vectors. The significant reduction of degrees of freedom leads to good stability of the algorithm.

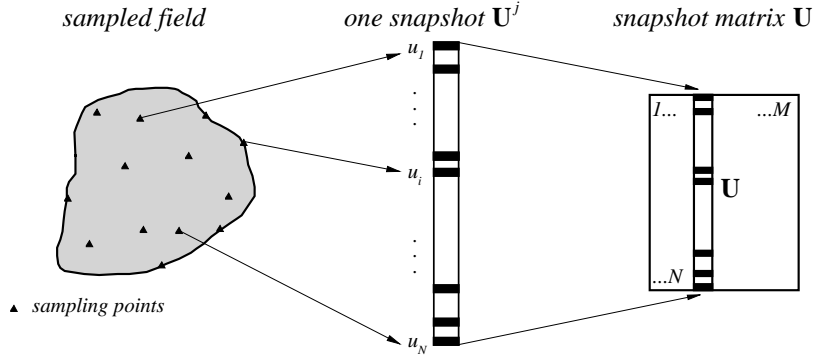


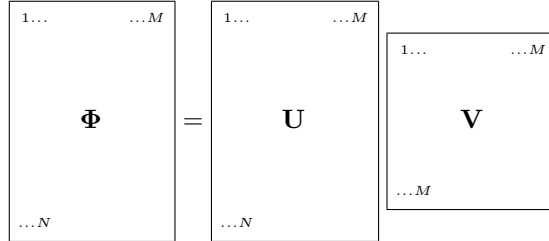
Figure 1: Idea of snapshots.

2. FUNDAMENTALS OF THE PROPER ORTHOGONAL DECOMPOSITION TECHNIQUE

The fundamental notion of POD is the *snapshot*, being a collection of N sampled values u_i of the field under consideration. The j^{th} snapshot is stored in a vector \mathbf{U}^j , $j = 1, 2, \dots, M$. The collection of snapshots, that are generated by changing some of parameter(s) upon which the field depends on, is stored in the rectangular N by M matrix \mathbf{U} . The sketch of a snapshot idea is presented in Figure 1. The snapshots may be obtained either by (numerical) simulation or from experiments. As already mentioned, the idea of POD has been re-developed several times starting from different viewpoints. The formulation based on the Karhunen-Loève transformation approach employing Sirovich snapshot technique is presented here.

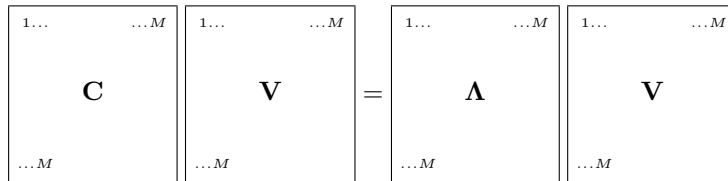
The aim of POD is to construct the set of orthonormal vectors (POD modes, POD basis vectors) Φ^j , $j = 1, 2, \dots, M$ resembling the original (snapshot) matrix \mathbf{U} in an optimal way. The elements of the basis are first expressed as a linear combination of the snapshots (Sirovich snapshot technique)

$$\Phi = \mathbf{U} \cdot \mathbf{V} \tag{1}$$



where \mathbf{V} stands for a modal matrix defined as a nontrivial solution of the following eigenvalue problem

$$\mathbf{C} \cdot \mathbf{V} = \Lambda \cdot \mathbf{V} \tag{2}$$



In the above Λ is a diagonal matrix storing the eigenvalues λ_i of the positive definite covariance matrix \mathbf{C} . The entries of the latter are defined as

$$\mathbf{C} = \mathbf{U}^T \cdot \mathbf{U} \tag{3}$$

$$\begin{array}{|c|} \hline 1 \dots \dots M \\ \hline \mathbf{C} \\ \hline \dots M \\ \hline \end{array} = \begin{array}{|c|} \hline 1 \dots \dots N \\ \hline \mathbf{U}^T \\ \hline \dots M \\ \hline \end{array} \begin{array}{|c|} \hline 1 \dots \dots M \\ \hline \mathbf{U} \\ \hline \dots N \\ \hline \end{array}$$

The eigenvalues are real and positive and should be sorted in a descending order.

It can be shown [3, 7], that if velocity is the field under consideration, the j^{th} eigenvalue is a measure of the kinetic energy transferred within corresponding (j^{th}) mode Φ^j . Typically, this energy decreases rapidly with the increasing number of the mode, which permits discarding the majority of modes. The truncation of the POD basis is accomplished by deciding which fraction of the energy may be neglected in further calculations. The resulting POD basis $\bar{\Phi}$, denoted as *truncated* POD basis, consists of $K < M$ elements (vectors):

$$\bar{\Phi} = \mathbf{U} \cdot \bar{\mathbf{V}} \quad (4)$$

$$\begin{array}{|c|} \hline 1 \dots \dots K \\ \hline \bar{\Phi} \\ \hline \dots N \\ \hline \end{array} = \begin{array}{|c|} \hline 1 \dots \dots M \\ \hline \mathbf{U} \\ \hline \dots N \\ \hline \end{array} \begin{array}{|c|} \hline 1 \dots \dots K \\ \hline \bar{\mathbf{V}} \\ \hline \dots M \\ \hline \end{array}$$

The truncated POD basis (4) is orthogonal $\bar{\Phi}^T \cdot \bar{\Phi} = \mathbf{I}$ and possesses optimal approximation properties. It can be shown that there is no other orthogonal basis that transfers more energy within the same number of modes.

Once the truncated POD basis is known, an arbitrary snapshot \mathbf{U}^a can be approximated as

$$\mathbf{U}^a = \bar{\Phi} \cdot \bar{\alpha}^a \quad (5)$$

$$\begin{array}{|c|} \hline 1 \dots \\ \hline \mathbf{U}^a \\ \hline \dots N \\ \hline \end{array} \approx \begin{array}{|c|} \hline 1 \dots \dots K \\ \hline \bar{\Phi} \\ \hline \dots N \\ \hline \end{array} \begin{array}{|c|} \hline 1 \dots \\ \hline \bar{\alpha}^a \\ \hline \dots K \\ \hline \end{array}$$

where $\bar{\alpha}^a$ stands for the amplitude vector associated with snapshot \mathbf{U}^a .

Equation (5) can be seen as an analog of Fourier expansion of the snapshot into a sequence of the POD vectors.

Resorting to the orthogonality of the truncated POD basis, the amplitude vector is evaluated from the equation

$$\bar{\alpha}^a = \bar{\Phi}^T \cdot \mathbf{U}^a \quad (6)$$

$$\begin{array}{|c|} \hline 1 \dots \\ \hline \bar{\alpha}^a \\ \hline \dots K \\ \hline \end{array} = \begin{array}{|c|} \hline 1 \dots \dots N \\ \hline \bar{\Phi}^T \\ \hline \dots K \\ \hline \end{array} \begin{array}{|c|} \hline 1 \dots \\ \hline \mathbf{U}^a \\ \hline \dots N \\ \hline \end{array}$$

The approximation formula (6) is, strictly speaking, valid only for snapshots that have been used to construct the POD basis. However, because the snapshots describe a behavior of a specific physical object, in practice the approximation holds also for arbitrary snapshots output by this object.

3. PROPOSED APPROACH

Let \mathbf{k} stand for a vector of the retrieved parameters. For the problem at hand, the entries of this vector are unknown conductivities and some values of the film coefficient at selected nodes located on the boundary.

The first step of the inverse procedure, is the generation of the snapshot matrix. This is accomplished by a numerical solution of a sequence of direct problems within the body under consideration. Taking some user defined values of the vector of the retrieved parameters \mathbf{k}^j , $j = 1, 2, \dots, M$, the inverse problem is transformed to a direct one, and as such can be solved using an arbitrary technique. The resulting temperature field is then sampled at a set of points and stored as a vector (snapshot) \mathbf{U}^j , $j = 1, 2, \dots, M$. All snapshots are stored as columns of the snapshot matrix \mathbf{U} . Once the matrix is generated, the truncated POD basis $\bar{\Phi}$ is constructed employing the already described technique.

In standard POD applications [4], the amplitude vectors $\bar{\alpha}^j$ are assumed to be constant. In the proposed approach, the amplitudes are allowed to be a nonlinear function of the vector of the retrieved parameters \mathbf{k} . Specifically, each amplitude is expressed as a linear combination of a vector (\mathbf{F}^j) being a set of predefined interpolation functions $f_i(\mathbf{k})$, i.e.

$$\mathbf{F}^j = \begin{bmatrix} f_1(\mathbf{k}^j) \\ \vdots \\ f_i(\mathbf{k}^j) \\ \vdots \\ f_m(\mathbf{k}^j) \end{bmatrix} \quad (7)$$

This yields to

$$\bar{\alpha}^j = \mathbf{B} \cdot \mathbf{F}^j \quad (8)$$

$$\begin{array}{|c|} \hline \dots \\ \hline \bar{\alpha}^j \\ \hline \dots K \\ \hline \end{array} = \begin{array}{|c|} \hline \dots & \dots M \\ \hline \mathbf{B} \\ \hline \dots K \\ \hline \end{array} \begin{array}{|c|} \hline \dots \\ \hline \mathbf{F}^j \\ \hline \dots M \\ \hline \end{array}$$

where the matrix \mathbf{B} contains unknown values of the coefficients of the combination.

The set of interpolation functions $f_i(\mathbf{k})$ can be chosen arbitrary, however some choices (e.g. monomials) could lead to ill-conditioned systems of equations that need to be solved in order to obtain the coefficient matrix \mathbf{B} .

In this study Radial Basis Functions (RBF) have been used as the interpolating functions. Due to their nice approximation and smoothing properties RBFs are often used in multidimensional approximation, pattern recognition etc. An overview of these functions is presented in [5, 6]. In the current study inverse multiquadric radial function have been employed. This kind of RBF function has a form

$$f_i(\mathbf{k}^j) = f_i(|\mathbf{k}^j - \mathbf{k}^i|) = \frac{1}{\sqrt{|\mathbf{k}^j - \mathbf{k}^i|^2 + r^2}} \quad (9)$$

where: r stands for user defined smoothing factor and \mathbf{k}^i , (also known as the node of the i^{th} RBF), is a known value of the \mathbf{k} vector. In the proposed approach, the nodes \mathbf{k}^i , $i = 1, 2, \dots, M$ of the RBFs are identical with the vectors \mathbf{k}^j , $j = 1, 2, \dots, M$ taken to generate the snapshots.

It can be seen, that the argument of the i^{th} RBF is the distance between its node and an arbitrary point \mathbf{k}^j .

To use efficiently approximation (8), the matrix \mathbf{B} should be evaluated. This can be accomplished by making this equation formula (8) exact for all snapshots that were used to generate the POD basis. This requirement leads to a matrix equation

$$\bar{\alpha} = \mathbf{B} \cdot \mathbf{F} \quad (10)$$

$$\begin{array}{|c|} \hline \dots & \dots M \\ \hline \bar{\alpha} \\ \hline \dots K \\ \hline \end{array} = \begin{array}{|c|} \hline \dots & \dots M \\ \hline \mathbf{B} \\ \hline \dots K \\ \hline \end{array} \begin{array}{|c|} \hline \dots & \dots M \\ \hline \mathbf{F} \\ \hline \dots M \\ \hline \end{array}$$

where: \mathbf{F} is the matrix of interpolation functions defined as

$$\mathbf{F} = \begin{bmatrix} f_1(|\mathbf{k}^1 - \mathbf{k}^1|) & \dots & f_1(|\mathbf{k}^j - \mathbf{k}^1|) & \dots & f_1(|\mathbf{k}^M - \mathbf{k}^1|) \\ \vdots & & \vdots & & \vdots \\ f_i(|\mathbf{k}^1 - \mathbf{k}^i|) & \dots & f_i(|\mathbf{k}^j - \mathbf{k}^i|) & \dots & f_i(|\mathbf{k}^M - \mathbf{k}^i|) \\ \vdots & & \vdots & & \vdots \\ f_M(|\mathbf{k}^1 - \mathbf{k}^M|) & \dots & f_M(|\mathbf{k}^j - \mathbf{k}^M|) & \dots & f_M(|\mathbf{k}^M - \mathbf{k}^M|) \end{bmatrix} \quad (11)$$

with $\mathbf{k}^i, \mathbf{k}^j$ - vectors of parameters used to generate i^{th} or j^{th} snapshot adequately, for $i, j = 1, \dots, M$.

The columns of matrix $\bar{\alpha}$ are the vectors of amplitudes corresponding to subsequent snapshots. It should be stressed that at this stage the matrix $\bar{\alpha}$ is known, as it can be evaluated from

$$\bar{\alpha} = \bar{\Phi}^T \cdot \mathbf{U} \quad (12)$$

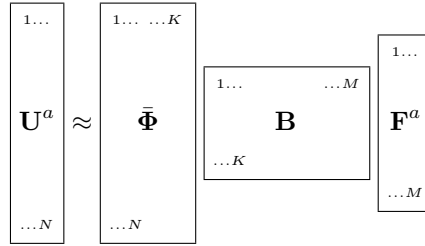
Transposition of (10) yields

$$\mathbf{F}^T \cdot \mathbf{B}^T = \bar{\alpha}^T \quad (13)$$

which is a set of linear equations with respect to the columns of matrix \mathbf{B}^T . Columns of the $\bar{\alpha}^T$ matrix are multiple right-hand side vectors of this set. If only the matrix \mathbf{F}^T is well behaved, solution of (13) presents no difficulty. Due to its nice numerical features, the Singular Value Decomposition [16] has been used at this stage.

After the coefficient matrix \mathbf{B} is evaluated, a low dimensional model of the temperature field (5) can be set as

$$\mathbf{U}^a \approx \bar{\Phi} \mathbf{B} \mathbf{F}^a \quad (14)$$



This model, hereafter referred to as the *trained RBF-POD network*, is capable of reproducing temperature fields that correspond to an arbitrary set of parameters \mathbf{k} . Obviously, extrapolation outside the range of \mathbf{k} which was used to generate snapshots, can lead to poor accuracy of the model.

4. INVERSE PROBLEM FORMULATION

The trained RBF-POD network (14) is used to retrieve the values of the unknown parameters \mathbf{k} . This is accomplished by resorting to the condition that the network should reproduce a set of measured temperatures in the least-square sense. Let $y_i, i = 1, \dots, m$ stand for the measured temperatures at some locations and $u_i^a, i = 1, \dots, m$ denote the values of the temperature at the same locations but calculated from model (14). The least squares objective function takes then a form

$$\Psi = \sum_{i=1}^m (u_i^a - y_i)^2 \quad (15)$$

The above least-squares problem can be solved by any technique (e.g. Levenberg-Marquardt, Genetic or Evolutionary Algorithm). The sketch of the inverse problem formulation is presented in Figure 2.

5. NUMERICAL EXAMPLES

Reference direct problem

A coated, internally cooled gas turbine blade is considered. The reference forward problem is defined as a 2D steady state temperature field with no internal heat generation and all boundary conditions known. The heat conductivities of the blade core and coating material (Thermal Barrier Coating - TBC), geometry and boundary conditions are depicted in Figure 3. Robin conditions are assumed along the external perimeter of the blade and inside the cooling holes. The film coefficient is assumed to be constant ($400 \text{ W/m}^2\text{K}$) inside the cooling holes, while along the outer boundary the known distribution

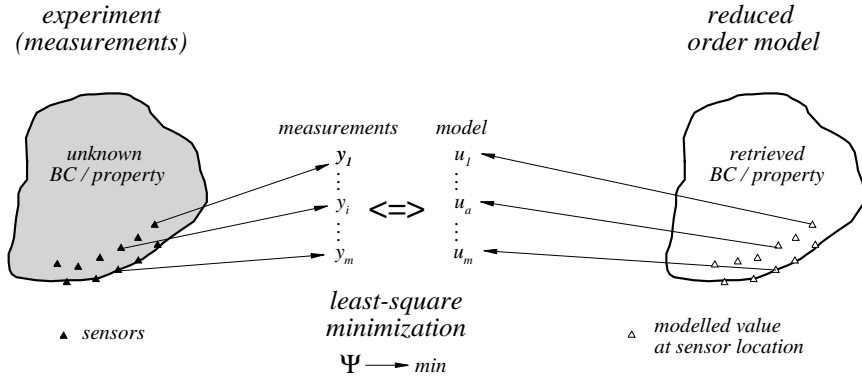


Figure 2: Inverse problem formulation.

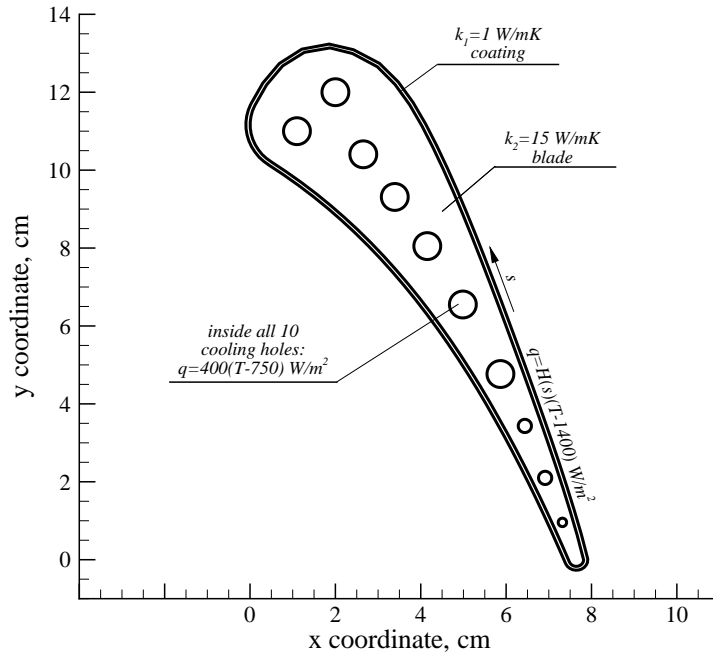


Figure 3: Geometry and boundary conditions.

is prescribed (see Figure 4). The direct problem has been solved using *MSC.Marc*, a FEM commercial code [11]. The numerical mesh consisted of 38772 quadratic (Tria 6) elements and 36497 nodes. The result of the forward problem was the temperature field in the domain under consideration.

Inverse problem

Inverse analysis has been conducted in the above described domain. The aim of the inverse analysis was to retrieve the unknown values of both constant heat conductivities (TBC, blade core) and the distribution of the film coefficient along the part of the external blade perimeter (see Figure 5).

The snapshots have been generated by solving a sequence of forward problems for different values of the retrieved parameters. The unknown distribution of the film coefficient has been described by a linear

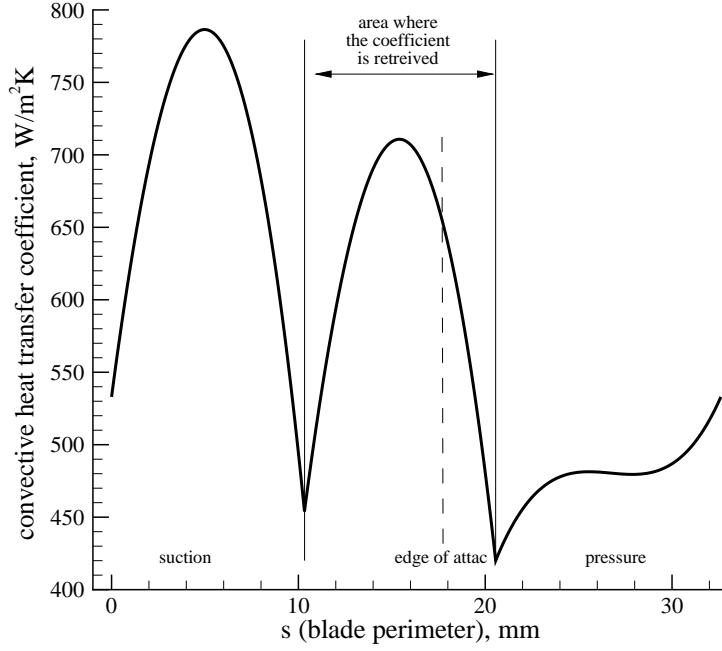


Figure 4: Film coefficient distribution along the external perimeter.

combination of Lagrange interpolating polynomials [18]

$$h(s) = \sum_{j=1}^n h_j H_j(s) \quad (16)$$

where

$$H_j(s) = \prod_{\substack{k=1 \\ k \neq j}}^n \frac{s - s_k}{s_j - s_k} \quad (17)$$

where s is the distance measured along the perimeters of the blade, s_j , s_k are nodes of the interpolation, h_j denotes the values of the heat transfer coefficient at these nodes and n stands for the number of interpolation nodes. In the study the value $n = 4$ has been taken.

With such formulation the dimensionality of the parameter vector \mathbf{k} is equal to 6 and the entries of this vector are defined as two conductivities (core and TBC) and values of the heat transfer coefficient at four nodes located on the boundary.

The snapshots were collections of 36497 nodal temperatures, total number of snapshots amounted to 729 for all possible combinations of parameters taken as:

- TCB conductivity: $k_1 = 0.6 \div 1.6$ W/mK with uniform interval of 0.33,
- blade core conductivity : $k_2 = 11.0 \div 21.0$ W/mK with uniform interval of 3.3,
- heat transfer coefficients h_j at Lagrange nodes taking values of: 400, 580, 760 and 940 W/m²K.

The POD basis has been generated assuming that 10^{-9} of the energy of the signal is neglected, and a truncated POD basis $\bar{\Phi}$ consisted of 11 vectors (modes). The values of subsequent eigenvalues associated with these vectors are: 4.26×10^{13} , 4.30×10^9 , 6.09×10^8 , 2.36×10^8 , 1.67×10^8 , 3.53×10^7 , 1.59×10^7 , 2.46×10^6 , 1.40×10^6 , 1.19×10^6 , 3.46×10^5 , 2.51×10^5 , 2.15×10^5 , 1.60×10^5 , 1.21×10^5 , 9.34×10^4 , 6.55×10^4 , 1.49×10^4 , 8.85×10^3 , 8.25×10^3 . The remaining were below 5.05×10^3 . Rapid decay of the eigenvalues confirms the strong correlation between the snapshots.

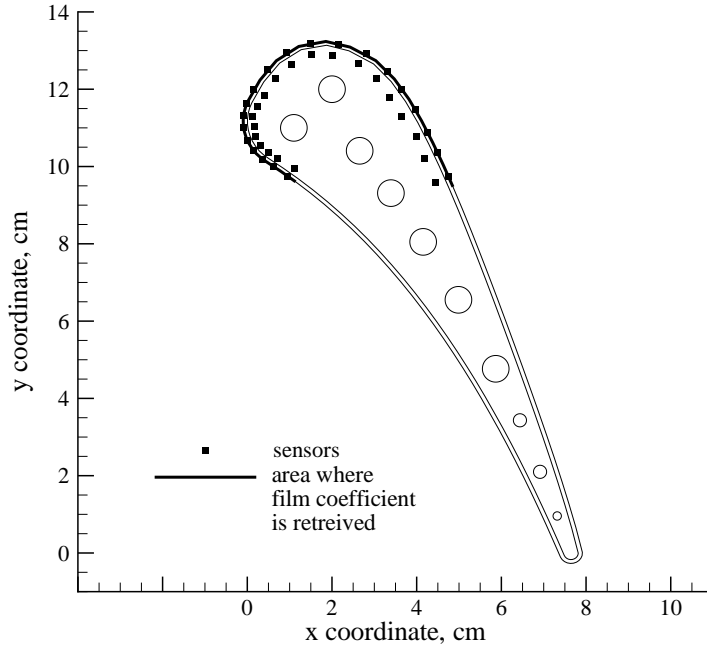


Figure 5: Location of the temperature sensors.

The *measurements* have been simulated by taking the temperatures obtained by a solution of the reference direct problem. Location of the sensors is shown in Figure 5. To simulate measurement error, a uniform random error of specified amplitude (0.1, 1.0, 2.0 and 5.0K) has been added to the temperature values. The distributed evolutionary algorithm was used to minimize the least-squares functional Ψ for $m = 40$ sensors (see Figure 5). Several tests runs made for every error level input data and starting from random population have been made. Best solutions were selected as the final result. The output of the inverse analysis concerning the heat conductivities is shown in Figure 6. The comparison between exact and estimated distribution of the film coefficient is shown in Figure 4.

At first sight the behavior of the error in Figure 7 might be considered strange. The best fit is obtained not for the unbiased *measurements*, but for the case of error amplitude equal to 2K. The explanation of this phenomenon lies in the much worse reproduction of the conductivity of the core material for the data set corresponding to the amplitude of the *measurement* error 2K.

Another striking feature of the results is that even using unbiased *measurements*, the exact distributions of the heat transfer coefficient and heat conductivities have not been obtained. This comes from the interpolation error committed when approximating the dependence of the amplitudes on the retrieved parameters vector \mathbf{k} by RBFs. This approximation is exact only at the selected values of the retrieved parameters \mathbf{k}_i . This interpolation error can be reduced by taking more sets of parameters (increase M). Another option is to repeat the entire analysis taking a new set of the parameter vectors located in the vicinity of the already obtained solution of the inverse problem.

6. CONCLUSIONS

The advances in the application of the trained POD inverse technique to the solution of complex inverse thermal problems have been presented. In the present paper the challenging task of simultaneous estimation of unknown heat conductivities and film coefficient distribution of the cooled turbine blade has been presented.

The most expensive portion of the analysis is the generation of the snapshots. It should be noted, that these computations can be very easily parallelized. As a single solution of the direct problem does not require data exchange with other computation units, the data transfer overhead is negligible.

The described technique has been used to solve several numerical examples [12] and proved to be a reliable and stable tool of solving inverse problems. This nice behavior can be attributed to the excellent

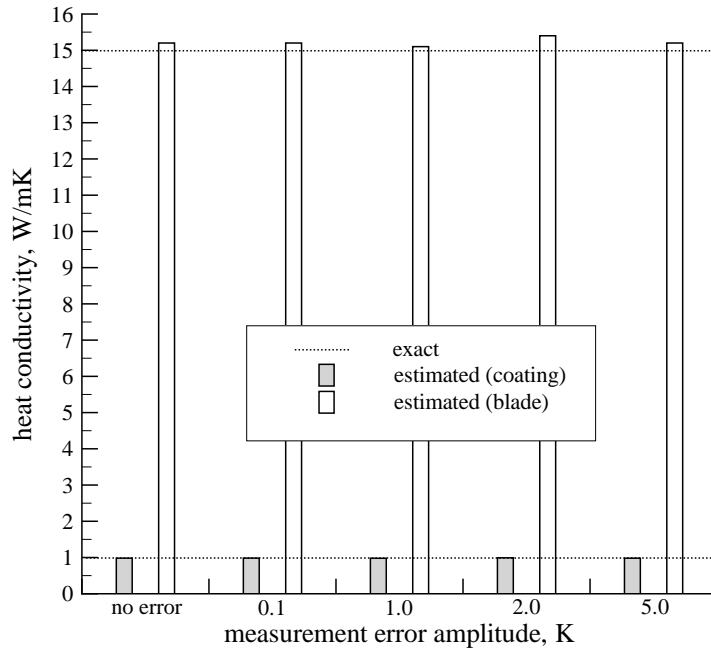


Figure 6: Estimated heat conductivities for blade and coating.

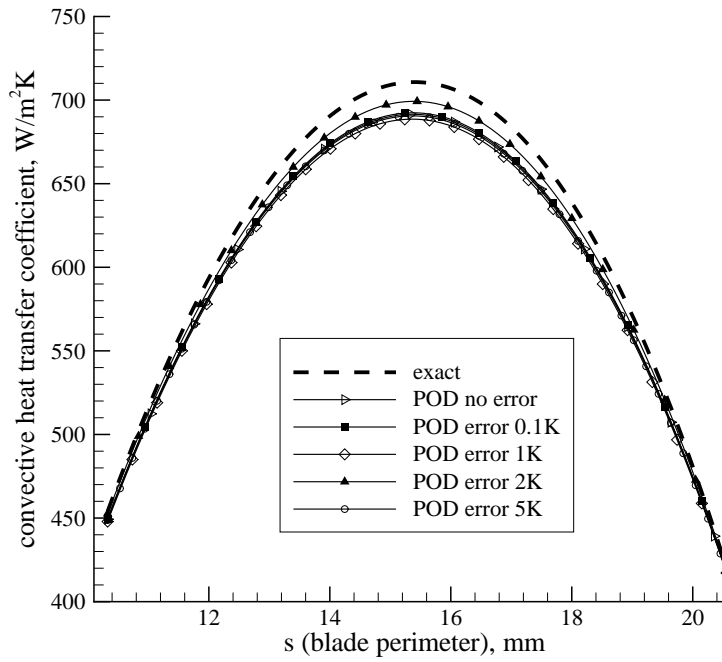


Figure 7: Estimated film coefficient distribution along the portion of the perimeter of the blade.

filtration properties of the POD basis which suppresses the high frequency noise.

Acknowledgments

Research of ZO and RAB has been financed by the Polish Committee for Scientific Research within the grant BW-459/RIE-6/2004. This help is gratefully acknowledged herewith. The authors wish to thank Dr Waclaw Kuś for providing them with his version of evolutionary algorithm.

REFERENCES

1. D. Ahlman, F. Soderlund, J. Jackson, A. Kurdila and W. Shyy, Proper orthogonal decomposition for time-dependent lid-driven cavity flows. *Num. Heat Transfer, Part B* (2002) **42**, 285–306.
2. J.V. Beck, B. Blackwell and C.R. St. Clair, *Inverse Heat Conduction: Ill-Posed Problems*, John Wiley and Sons, New York, 1985.
3. G. Berkooz, P. Holmes and J.L. Lumley, The proper orthogonal decomposition in the analysis of turbulent flows, *Ann. Rev. Fluid Mech.* (1993) **25**(5), 539–575.
4. R.A. Bialecki, A.J. Kassab and Z. Ostrowski, Application of the proper orthogonal decomposition in steady state inverse problems, *Inverse Problems in Engineering Mechanics IV*, (ed. M. Tanaka), Elsevier BV, Amsterdam, 2003, pp.3–12.
5. R.L. Hardy, Multiquadric equations of topography and other irregular surfaces. *J. Geophys. Res.* (1971) **76**, 1905–1915.
6. R.L. Hardy, Theory and applications of the multiquadric-biharmonic method: 20 years of discovery 1968-1988. *Comput. Math. Appl.* (1990) **19**(8-9), 163-208.
7. P. Hølems, J.L. Lumley and G. Berkoz, *Turbulence, Coherent Structures, Dynamical Systems and Symmetry*, Cambridge Monographs on Mechanics, Cambridge University Press, Cambridge, 1996.
8. M. Kirby and L. Sirovich, Application of Karhunen-Loève procedure for characterization of human faces. *IEEE Trans. Pattern Anal. Machine Intelligence* (1990) **12**(1), 103–108.
9. Y.C. Liang, H.P. Lee, S.P. Lim, W.Z. Lin, K.H. Lee and C.G. Wu, Proper orthogonal decomposition and its applications - Part I: Theory. *J. Sound Vibr.* (2002) **252**(3), 527–544.
10. H.V. Ly and H.T. Tran, Modelling and control of physical process using proper orthogonal decomposition. *Math. Comput. Model.* (2001) **33**, 223–236.
11. MSC.Software Corporation, <http://www.mscsoftware.com>.
12. Z. Ostrowski, *Application of Proper Orthogonal Decomposition to the Inverse Problems*, PhD thesis, Silesian University of Technology, Gliwice, 2005.
13. Z. Ostrowski, R.A. Bialecki and A.J. Kassab, Estimation of constant thermal conductivity by use of proper orthogonal decomposition, *International Association for Boundary Element Methods 2004 Conference (IABEM 2004)*, University of Minnesota-Twin Cities, USA, 2004, ext. abstract book.
14. M.N. Özisik and H.R.B. Orlande, *Inverse Heat Transfer: Fundamentals and Applications*, Taylor & Francis, New York, 2000.
15. K. Pearson, On lines planes of closes fit to system of points in space. *The London, Edinburgh and Dublin Philosophical Magazine and J. Sci.* (1901) **2**, 559–572.
16. W.H. Press, S.A. Teukolsky, W.T. Vetterling and B.P. Flannery, *Numerical Recipes in FORTRAN: The Art of Scientific Computing*, Cambridge University Press, Cambridge, 1992.
17. A.N. Tikhonov and V.A. Arsenin, *Solution of Ill-Posed Problems*, John Willey and Sons, New York, 1977.
18. E.W. Weisstein, *Lagrange Interpolating Polynomial*, from MathWorld—A Wolfram Web Resource, <http://mathworld.wolfram.com/LagrangeInterpolatingPolynomial.html>.
19. C.G. Wu, Y.C. Liang, W.Z. Lin, H.P. Lee and S.P. Lim, A note on equivalence of proper orthogonal decomposition methods. *J. Sound Vibr.* (2003) **265**, 1103–1110.